Some comparisons between linear and non linear horizontal diffusion schemes for the ECMWF grid point model

R. Strüfing

Research Department

June 1982

Abstract

Two series of forecasts with the ECMWF Grid Point Model have been carried out in order to compare the performance of a fourth order horizontal diffusion scheme with that of a non-linear second order scheme (Smagorinsky, 1963). For the period for which the forecasts are skillful the differences between the two series are marginal. However, by day 10 the linear fourth order scheme is slightly superior, mainly because it forecasts the very long waves, wavenumbers 1-3, more accurately. In contrast to this the non-linear second order diffusion scheme often produces lows which are more shallow and which are closer to reality. A 30 day integration from 1.1.77 showed that extended range forecasts are not very sensitive to the choice of order of the horizontal diffusion schemes. In this case both ECMWF forecasts were not able to match the performance of the GFDL model.

1
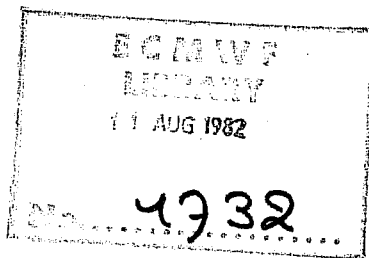
model. Since the GFDL model uses a non-linear second order scheme for the horizontal diffusion this scheme has been implemented into the ECMWF model and a series of forecasts undertaken in order to evaluate the impact of the horizontal diffusion on the differences between GFDL and ECMWF forecasts in the 1.1.77 case.

2. FORMULATION OF THE GFDL NON-LINEAR SECOND ORDER HORIZONTAL DIFFUSION SCHEME

2.1 Continuous equations

The approach follows that of Smagorinsky (1963). The horizontal diffusion terms $_HF_u$, $_HF_v$, $_HF_T$ and $_HF_q$ for the two components of the momentum equations, the thermodynamic equation and the equations for conservation of moisture, respectively and written as:

$$p_s \; _HF_u \; = \; \frac{1}{a\cos\theta} \; \frac{\partial}{\partial\lambda} \; (\tau_{\lambda\lambda}) + \frac{1}{a\cos^2\theta} \; \frac{\partial}{\partial\theta} \; (\tau_{\lambda\lambda} \cos^2\theta) \tag{1}$$

$$p_s \; _HF_v \; = \; \frac{1}{a\cos\theta} \; \frac{\partial}{\partial\lambda} \; (\tau_{\theta\lambda}) + \frac{1}{a\cos\theta} \; \frac{\partial}{\partial\theta} \; (\tau_{\lambda\lambda} \cos\theta) + \frac{\tan\theta}{a} \; \tau_{\lambda\lambda} \tag{2}$$

$$p_s \; _HF_T \; = \; \frac{1}{a\cos\theta} \; \frac{\partial}{\partial\lambda} \; (p_s\Gamma \; \frac{1}{a\cos\theta} \; \frac{\partial\Gamma}{\partial\lambda}) + \frac{1}{a\cos\theta} \; \frac{\partial}{\partial\theta} \; (p_s \; \Gamma\cos\theta\frac{1}{a} \; \frac{\partial\Gamma}{\partial\theta}) \tag{3}$$

$$p_s \; _HF_q \; = \; \frac{1}{a\cos\theta} \; \frac{\partial}{\partial\lambda} \; (p_s\Gamma \; \frac{1}{a\cos\theta} \; \frac{\partial q}{\partial\lambda}) + \frac{1}{a\cos\theta} \; \frac{\partial}{\partial\theta} \; (p_s\Gamma \; \cos\theta\frac{1}{a} \; \frac{\partial q}{\partial\theta}) \tag{4}$$

The stress terms $\tau_{\lambda\lambda}$, $\tau_{\lambda\theta}$, $\tau_{\theta\lambda}$ and $\tau_{\theta\theta}$ are defined in terms of the deformation fields associated with the horizontal velocities. We express $\tau_{\lambda\lambda}$, $\tau_{\lambda\theta}$ by

and

$$D^2 = D_r^2 + D_s^2 \tag{11}$$

Assuming $\Gamma = \gamma$ equations (1) - (4) can be rewritten:

$$p_s \, {}_H F_u = 2(k_o a\Delta\theta)^2 \frac{1}{a\cos\theta} \left[\frac{\partial}{\partial\lambda} (p_s \, n \, |D|D_r) + \frac{1}{\cos\theta} \frac{\partial}{\partial\theta} (p_s n |D| D_s \cos^2\theta) \right] \tag{12}$$

$$p_s \, {}_H F_v = 2(k_o a\Delta\theta)^2 \frac{1}{a\cos\theta} \left[\frac{\partial}{\partial\lambda} (p_s \, n \, |D|D_s) - \frac{1}{a\cos\theta} \frac{\partial}{\partial\theta} (p_s n |D| D_r \cos^2\theta) \right] \tag{13}$$

$$p_s \, {}_H F_T = 2(k_o a\Delta\theta)^2 \frac{1}{a\cos\theta} \left[\frac{\partial}{\partial\lambda} (p_s \, n \, |D|\frac{\partial\Gamma}{\partial\lambda}) + \frac{\partial}{\partial\theta} (p_s n |D|\frac{\partial\Gamma}{\partial\theta}) \right] \tag{14}$$

$$p_s \, {}_H F_q = 2(k_o a\Delta\theta)^2 \frac{1}{a\cos\theta} \left[\frac{\partial}{\partial\lambda} (p_s n |D| \frac{\partial q}{\partial\lambda}) + \frac{\partial}{\partial\theta} (p_s n |D| \frac{\partial q}{\partial\theta}) \right] \tag{15}$$

The notation used is that adopted in the ECMWF Forecast Model Documentation (1981).

2.2 Discretization

In the ECMWF grid point model the primitive equations are formulated for a C-grid illustrated in Fig. 1.

The variations of p_s are not considered here in order to save computer time. Similarly $|D|$ is calculated using

$$|D|^T = |D_s| + |D_r|^{-\lambda\theta} \qquad |D|^S = |D_s| + |D_r|^{-\lambda\theta}$$

$$|D|^u = |D_s|^{-\theta} + |D_r|^{-\lambda} \qquad |D|^v = |D_s|^{-\lambda} + |D_r|^{-\theta} \qquad (20)$$

The deformation terms are given by

$$D_s = \frac{1}{a\cos\theta} \delta_\lambda v + \frac{\cos\theta}{a} \delta_\theta \left(\frac{u}{\cos\theta}\right) \qquad (21)$$

$$D_r = \frac{1}{a\cos\theta} \delta_\lambda u - \frac{\cos\theta}{a} \delta_\theta \left(\frac{v}{\cos\theta}\right) \qquad (22)$$

at $\theta = \pm \pi/2 \mp \Delta\theta/2$

D_s has to be modified at $\theta = \pm \frac{\pi}{2} \mp \frac{\Delta\theta}{2}$, because $u/\cos\theta$ is not defined at the poles

$$D_s \left(\pm \frac{\pi}{2} \mp \frac{\Delta\theta}{2}\right) = \frac{1}{a\cos\theta} (\delta_\lambda v + u \sin\theta)^{-\theta} + \frac{1}{a} \delta_\theta u \qquad (23)$$

at $\theta = \pm \pi/2$

The velocity u has to be calculated for the polar rows using the surface pressure tendency equation over the polar cap. At the poles D_T is given by

3. SUBJECTIVE AND OBJECTIVE ASSESSMENT

In this study five 10-day forecasts have been carried out for initial data of
the 16.1.79, 1.3.65, 12.2.81, 5.4.81 and 1.1.177 with each diffusion scheme.
The forecast from the latter date was extended to 30 days. In addition
results of GFDL forecasts are available for the 1.3.65 (1967 version
(Miyakoda et al, 1974)) the 1.1.77 (GFDL model with higher order closure
vertical diffusion (Miyakoda et al, 1980))

In the following the linear fourth order diffusion will be referred to as L4
and the second order non-linear scheme as NL2.

3.1 Selection of the van Karman constant for NL2

Three forecasts from the 16.1.79 were made with the non-linear second order
scheme using different diffusion coefficients in order to optimize the
performance of NL2. The anomaly-correlations in the geopotential height
fields (Fig. 2) indicate that integrations with k_o = .2 are slightly superior
to $k_{o=}$ .3.

3.2. Synoptic evaluation

This assessment is mainly based on the 500 and 1000 mb geopotential height
fields at day 10 as well as on the time evolution of the anomaly-correlations
of height in the troposphere. Separate correlations of amplitude and phase
are not considered here, because they showed no significant differences.

(i) 16.1.79 10-day forecast

Fig. 3a-b illustrates the geopotential height fields. The L4 forecast is
very similar to that of NL2 even out to day 10. Significant differences can
only be found in the lows over Europe and the West-Pacific. These systems
seem less developed in the NL2 scheme and are indeed closer to the verifying
analysis. However, the anomaly correlations (Fig.4) indicate an advantage

9

well as 4-9.

(v) 1.1.1977 10-day forecast

The results of the forecast from this dataset are illustrated in Fig.11a-b
and 12. The GFDL model performs better than the two ECMWF models mainly
because it captures well the two ridges over the Rocky Mountains and the
Atlantic, the first only weakly indicated by the two ECMWF forecasts. As in
the case of 12.2.81 the anomaly correlations for the waves 1-3 are marginally
better for NL2 in the range of useful predictability.

(vi) 1.1.1977 30-day forecast

The 10-day forecasts have been extended to 30 days in order to compare the
results with a monthly forecast made with the GFDL model (Miyakoda et al,
1980). Running the ECMWF model with NL2 diffusion using the space filter of
chopping of total tendencies led to non-linear instability at the south pole
after 18 days. The forecast was successfully started from day 10 with a
modified E-W smoothing used with the L4 diffusion. This replaces the
tendency chopping and was designed to be especially effective near the poles.

The results of these monthly integrations are presented by means of
geopotential height fields averaged over the last 10 days and the full length
of the 30 days (Fig.13a-b and 14a-b). The mean charts of the last 10 days of
the integration clearly indicate that for a high resolution model the choice
of horizontal diffusion schemes is of little importance, even for extended
range forecasts.

The major phase difference is in the Pacific with the NL2 scheme having a
larger eastward shift of the Aleutian low. Also the L4 diffusion simulates a
cut-off low over East Russia which indicates the only major difference in
amplitude. The tendency of the NL2 scheme to produce less pronounced surface

11

Rainfall maps not presented here indicate slightly increased large-scale precipitation for the latitudes with stronger cooling but no other systematic differences between the two diffusion schemes could be found.

4. CONCLUSIONS

Using the N48 ECMWF gridpoint model two horizontal diffusion schemes have been compared; one being the standard linear fourth order diffusion, the other the GFDL-type non-linear second order scheme. For a 10-day forecast period the results obtained with both schemes were very similar and even a monthly integration did not show significant differences. Some forecasts have been compared with the results of the GFDL model, but it was not possible to show that one of the ECMWF models was significantly closer to the GFDL model.

Although the differences between the models were small it was found in agreement with Williamson (1978) that the linear fourth order diffusion generally showed higher scores, in particular the anomaly correlation for the wavenumbers 1-3 was better. The advantage of the non-linear second order scheme was that it often produced a less deep development of surface lows.

These results indicate that for extended range forecasts the choice of diffusion is less important and does not contribute essentially towards the differences in the results obtained by the ECMWF and GFDL models in the case of the 30-day integration from the 1.1.77. The same was found for the difference between energy and enstrophy conservation (Strüfing, 1982). In view of the major differences in subgrid scale parameterization schemes, a higher closure vertical diffusion scheme is to be implemented into the physics of the ECMWF grid-point model.
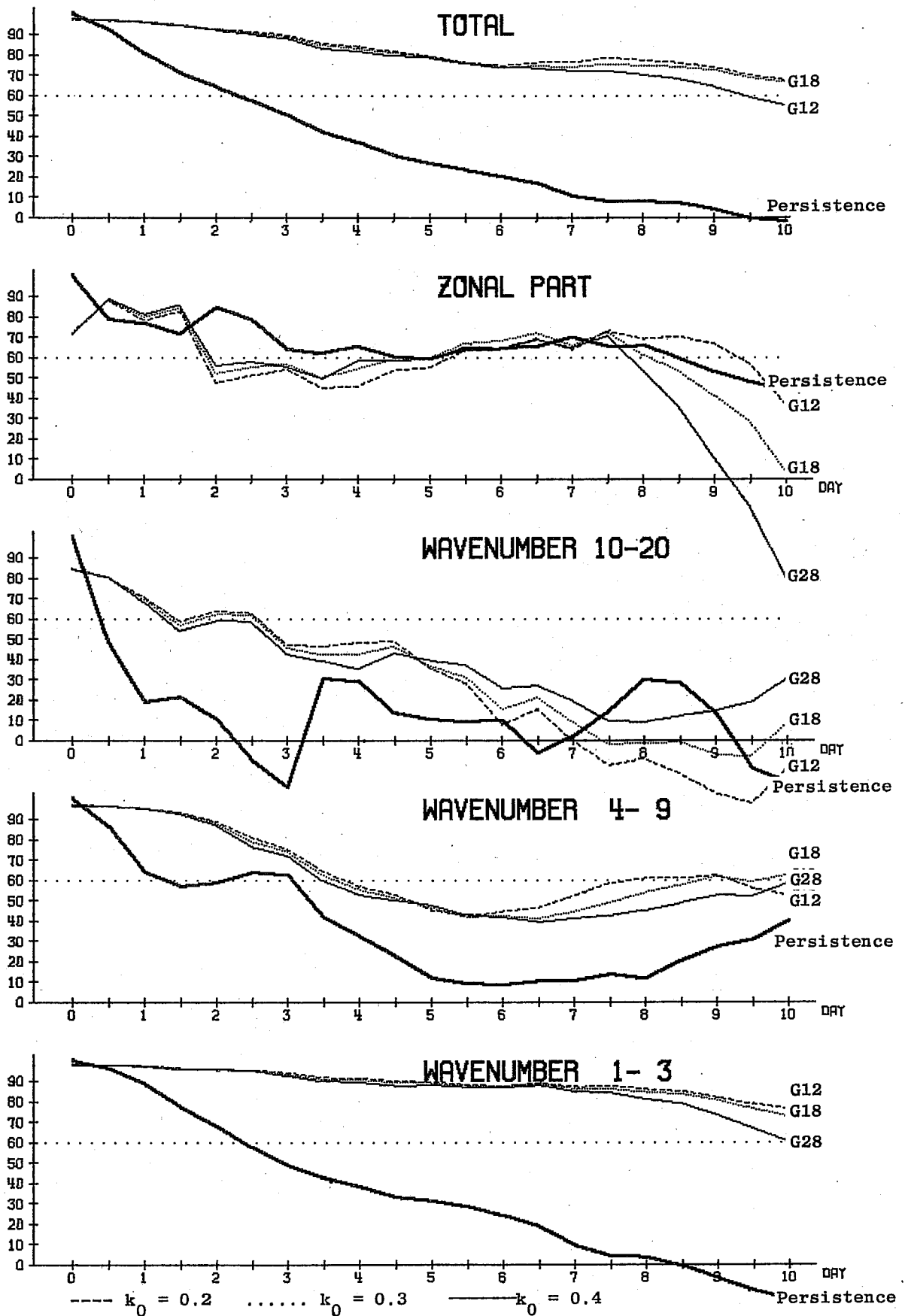
Fig. 2 Anomaly correlation coefficients of the geopotential height field for
the forecast from 16.1.79. for the NL2 scheme with various diffusion
coefficients. Mean for troposphere 200-1000 mb and 20°-82.5°N.
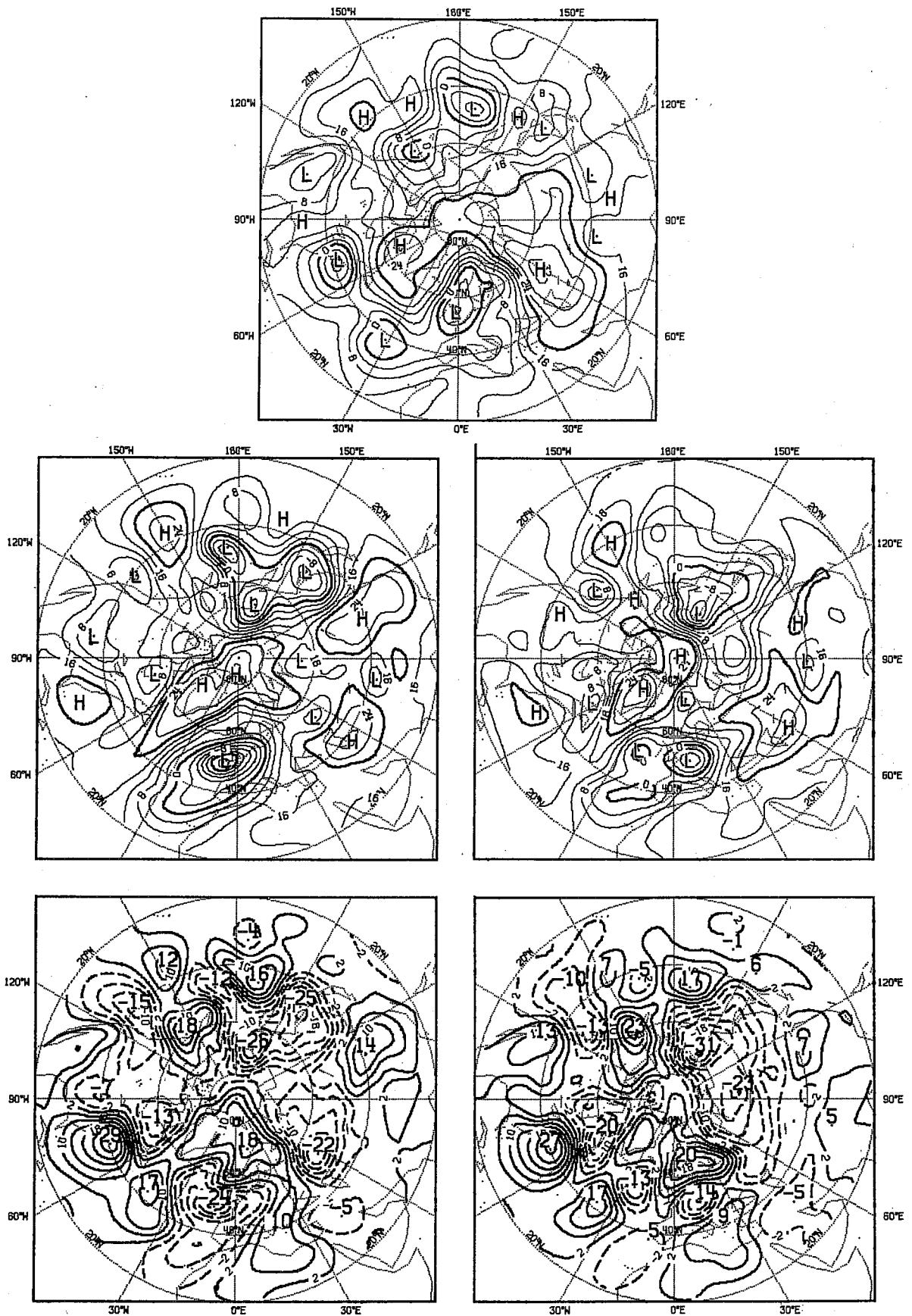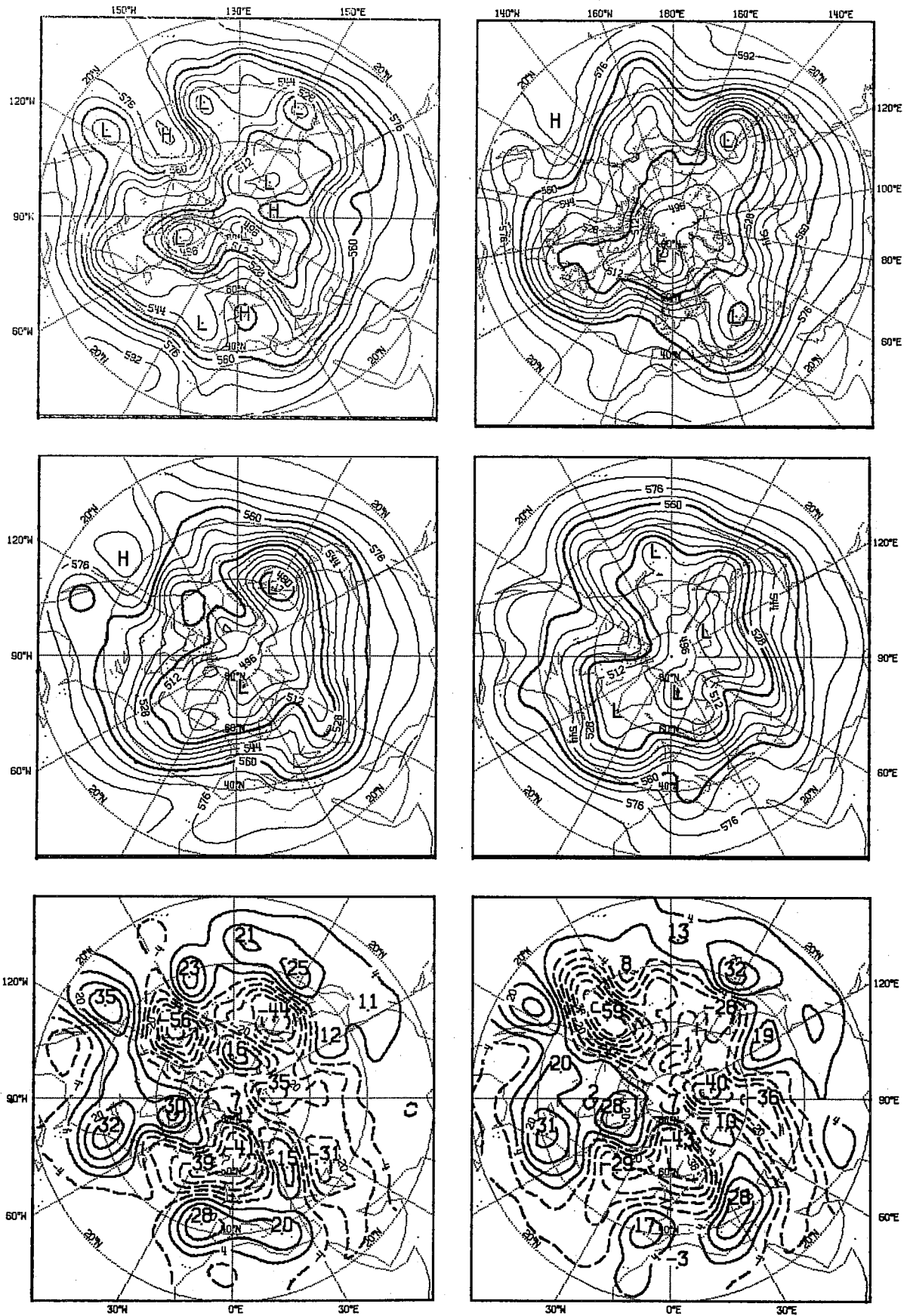
Fig. 3b As for Fig. 3a but for 1000 mb.

Fig. 5a Northern hemisphere geopotential height fields for 500 mb at Day 10
for verifying analysis (top left); GFDL forecast (top right); ECMWF
forecasts with L 4 (centre left) and N L 2 (centre right from
1.3.65. and differences to verifying analysis (bottom).
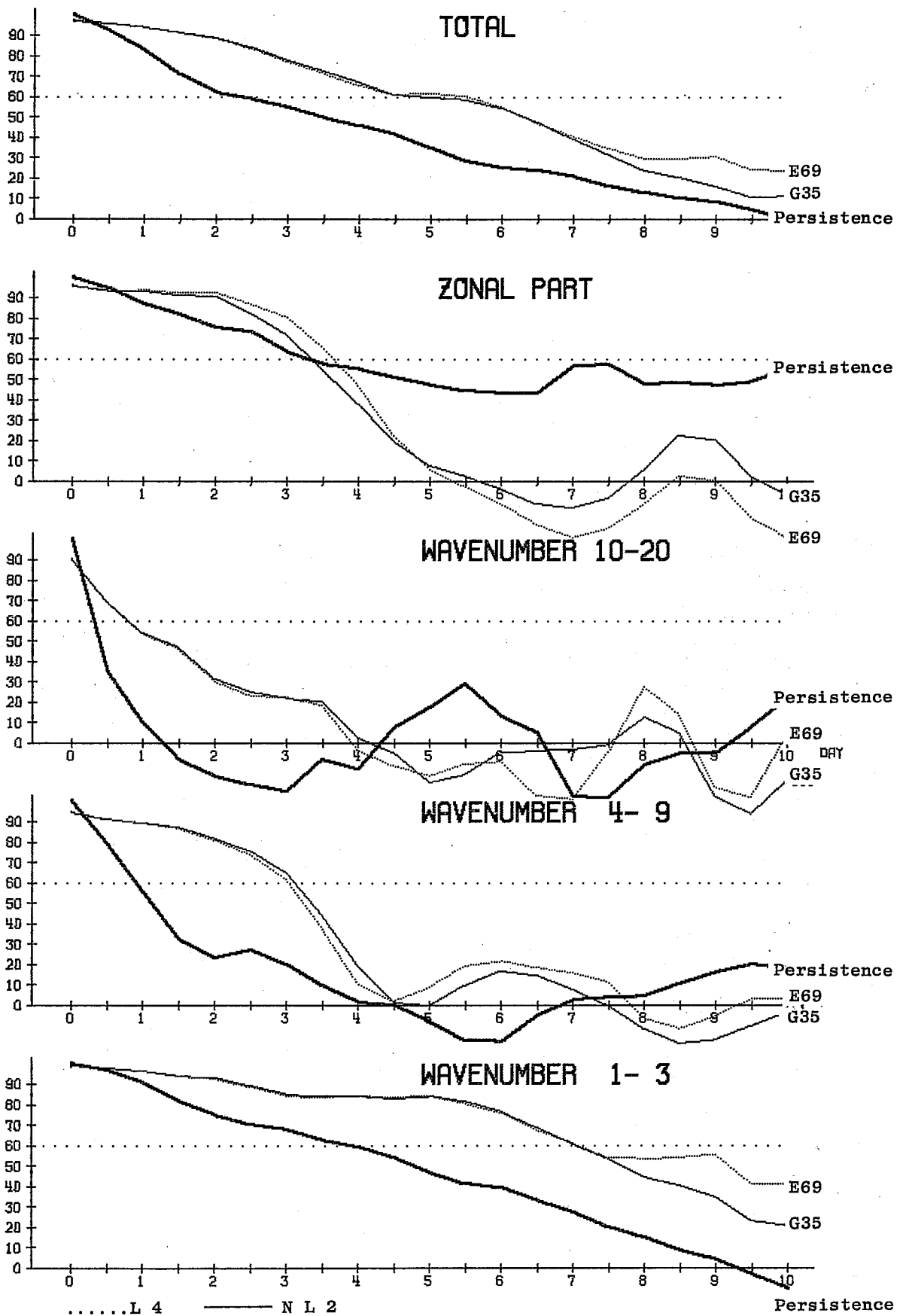
Fig. 6 As for Fig. 4 but for 1.3.65.
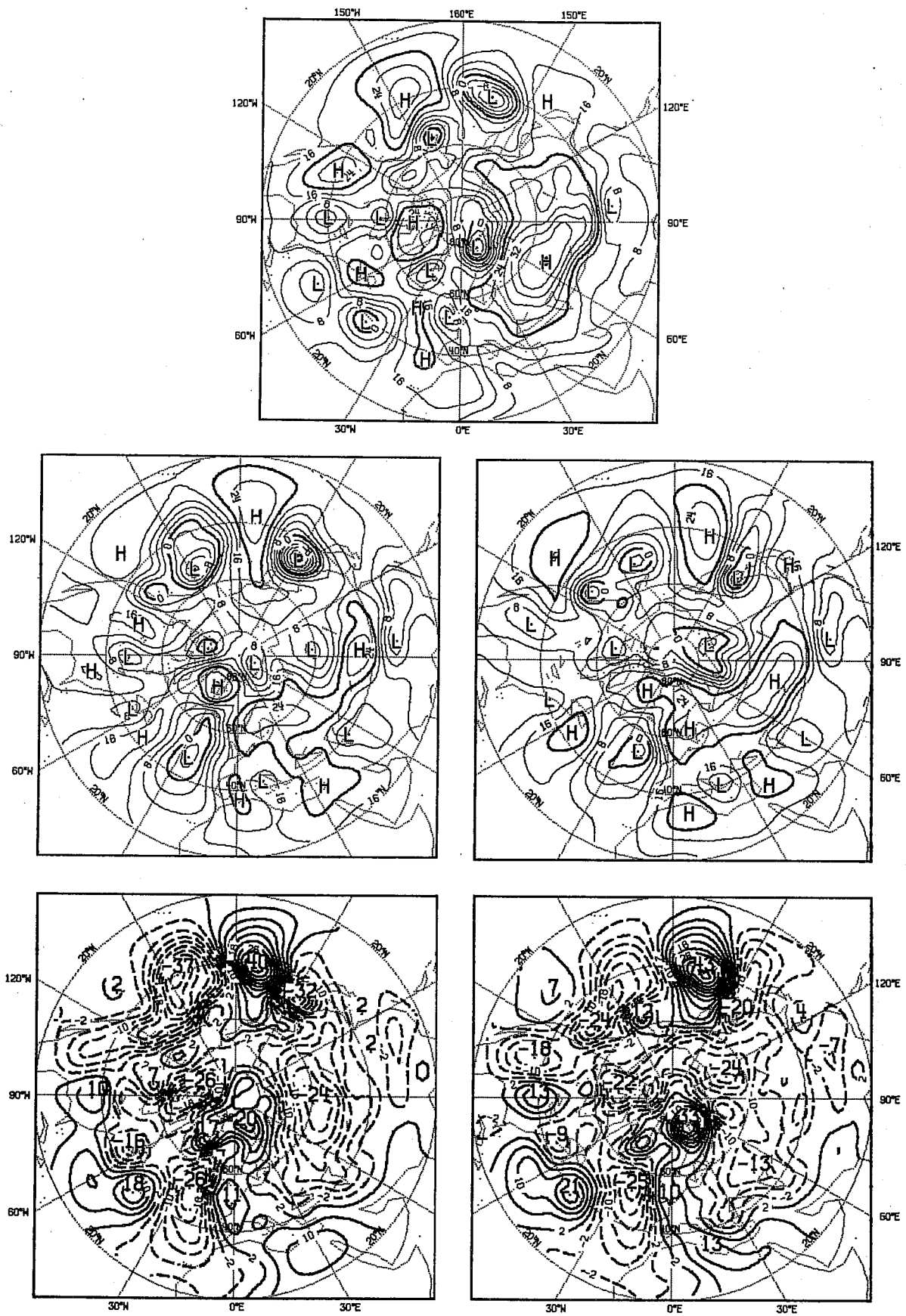
Fig. 7b   As for Fig. 3b but for 22.2.81.
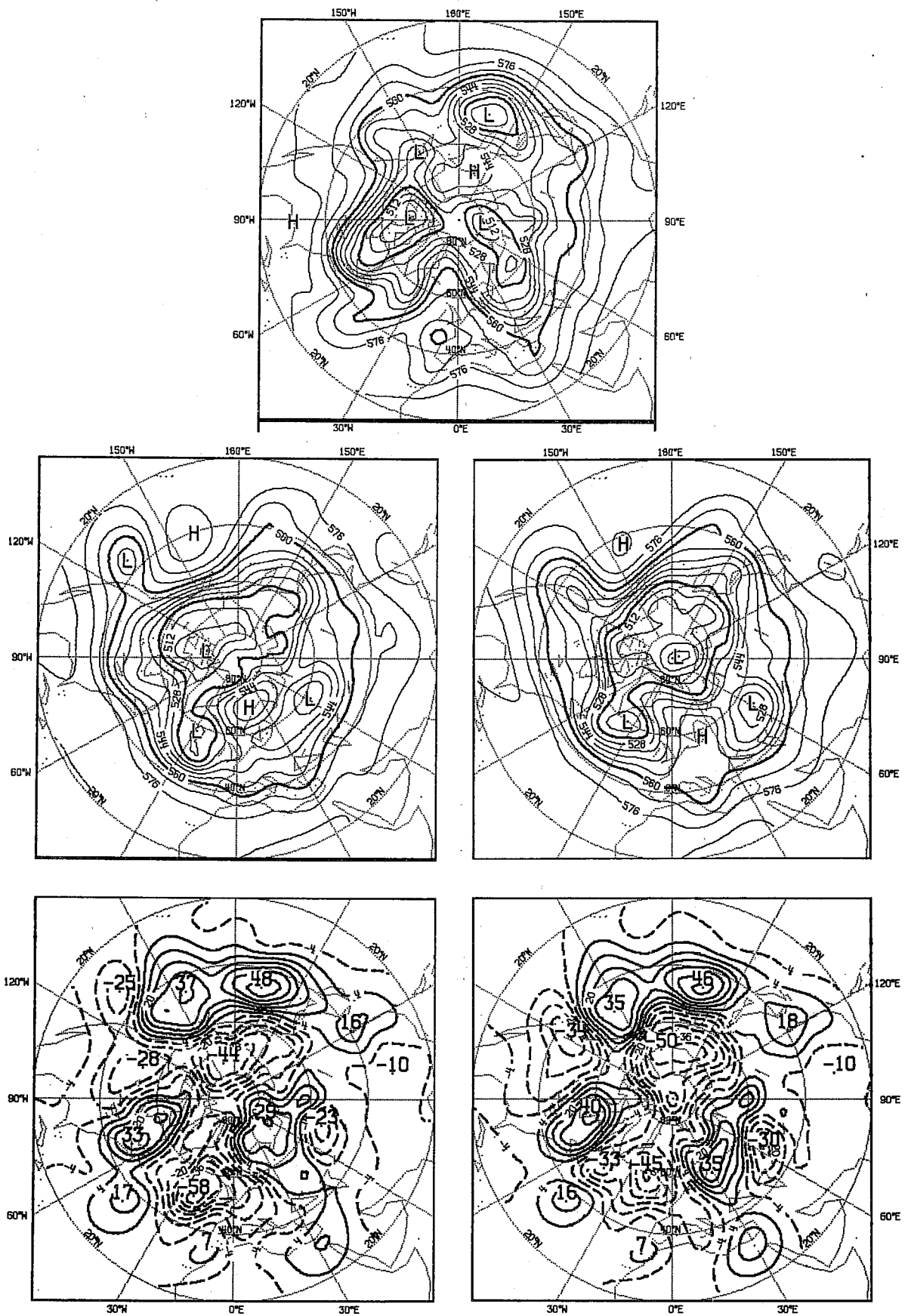
Fig. 9a   As for Fig. 3a but for 5.4.81.
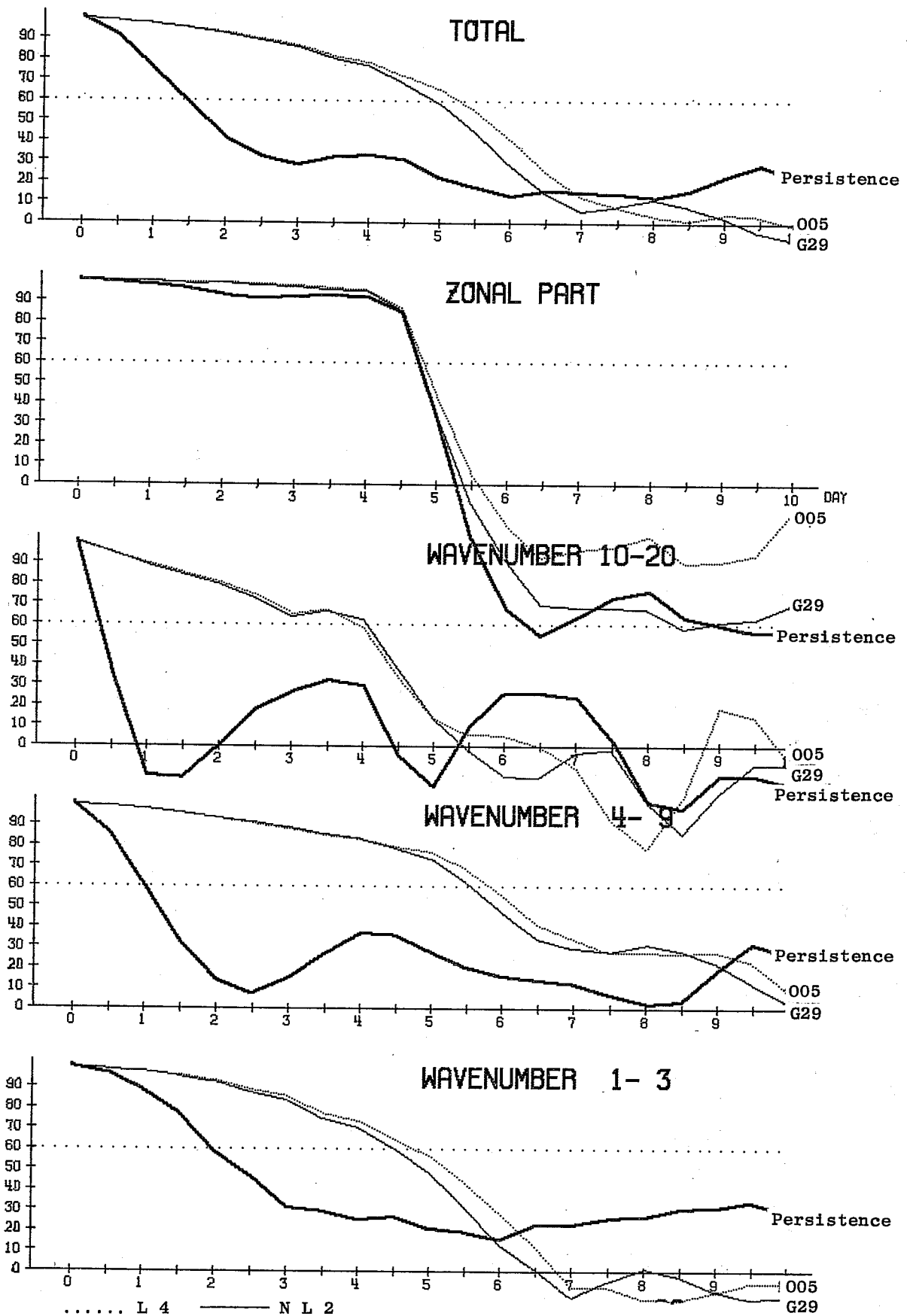
Fig. 10   As for Fig. 4 but for 5.4.81.
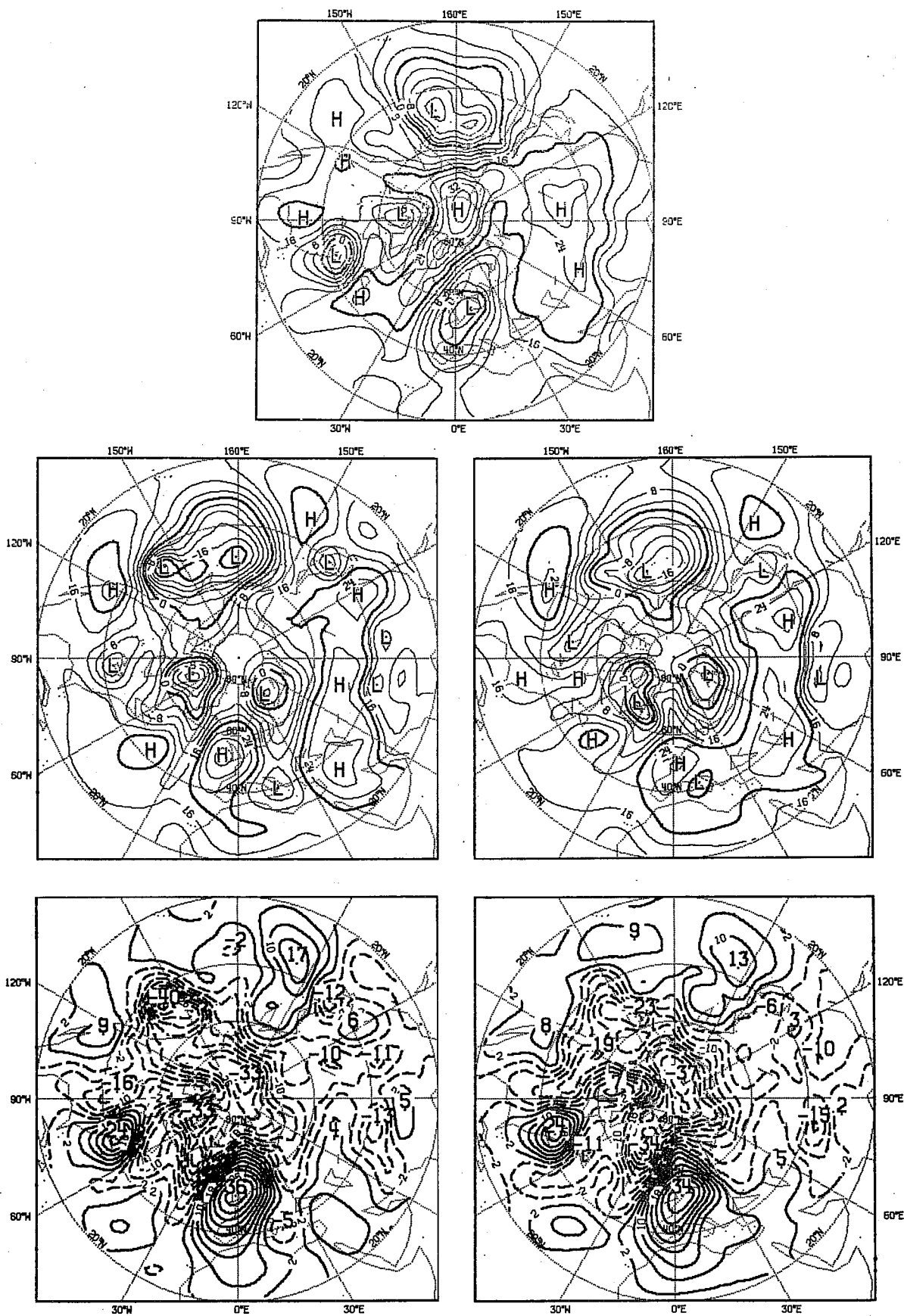
Fig. 11b   As for Fig. 3b but for 1.1.77.
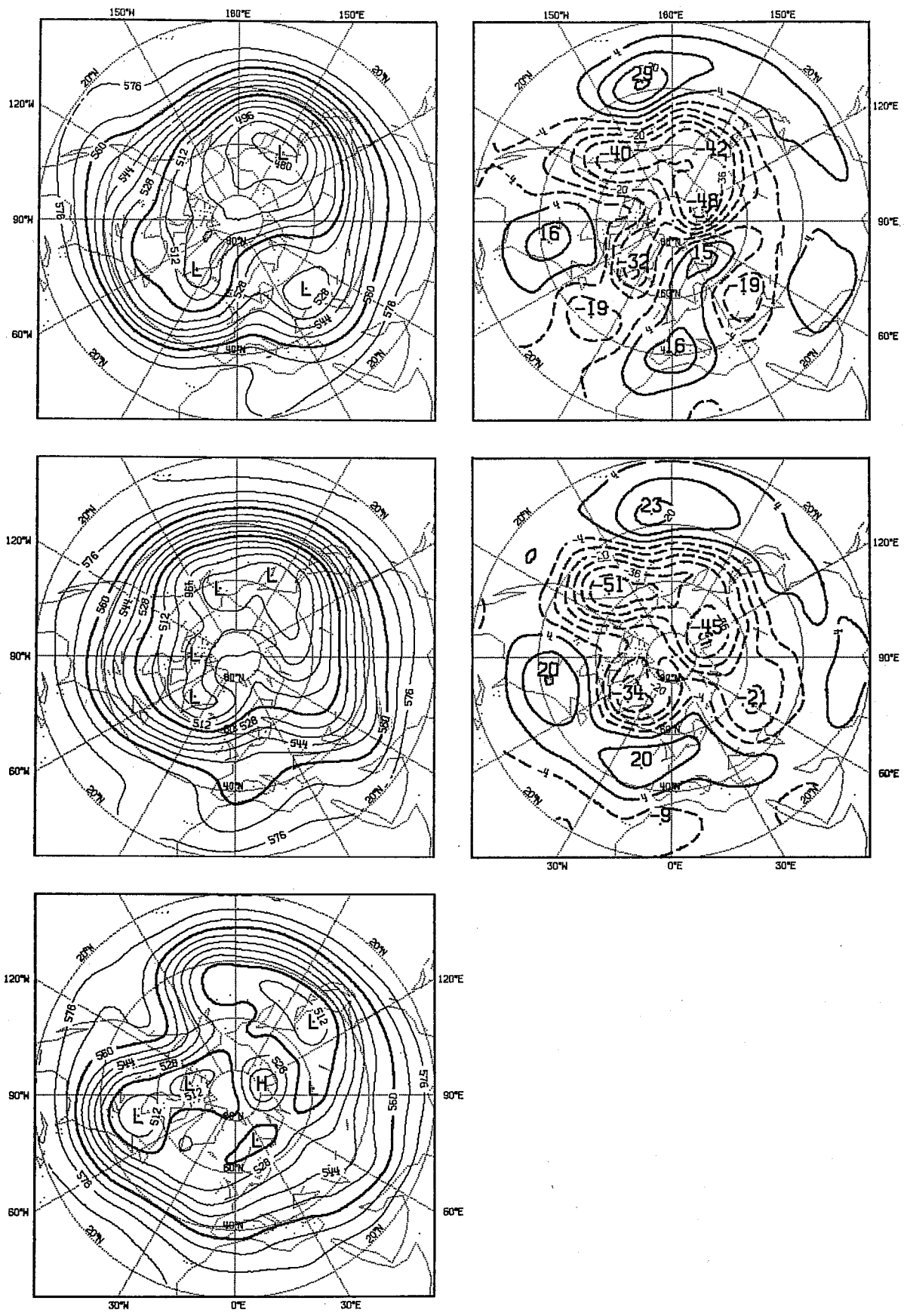
Fig. 13a 10 day mean northern hemisphere geopotential height fields (right)
for 500 mb for Day 21 to 30 from 1.1.77. got L 4 (top); N L 2
diffusion (centre) forecasts; verifying analysis (bottom) and
differences forecast analysis (left).
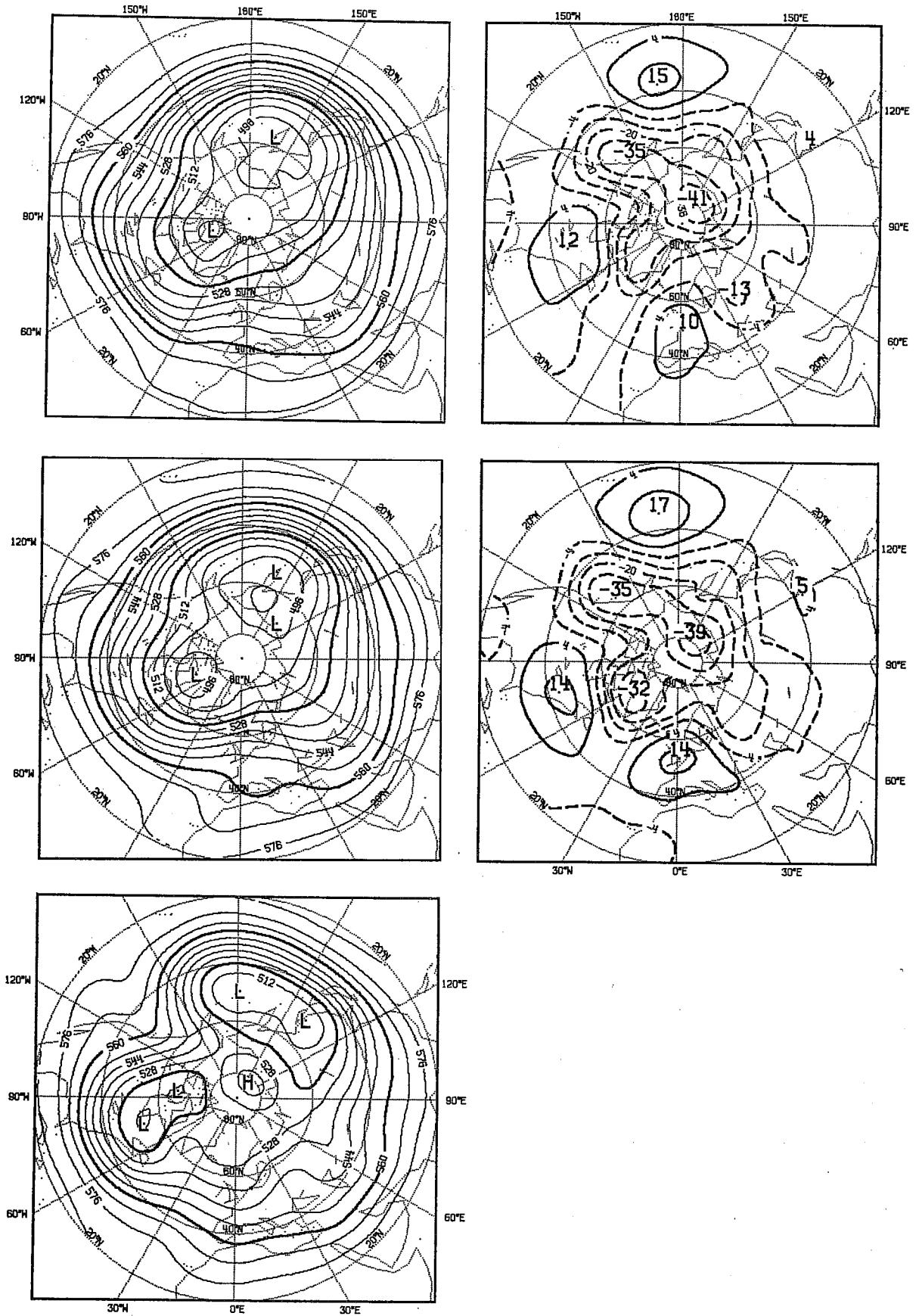
Fig. 14a As for Fig. 13a but for 30 day mean.

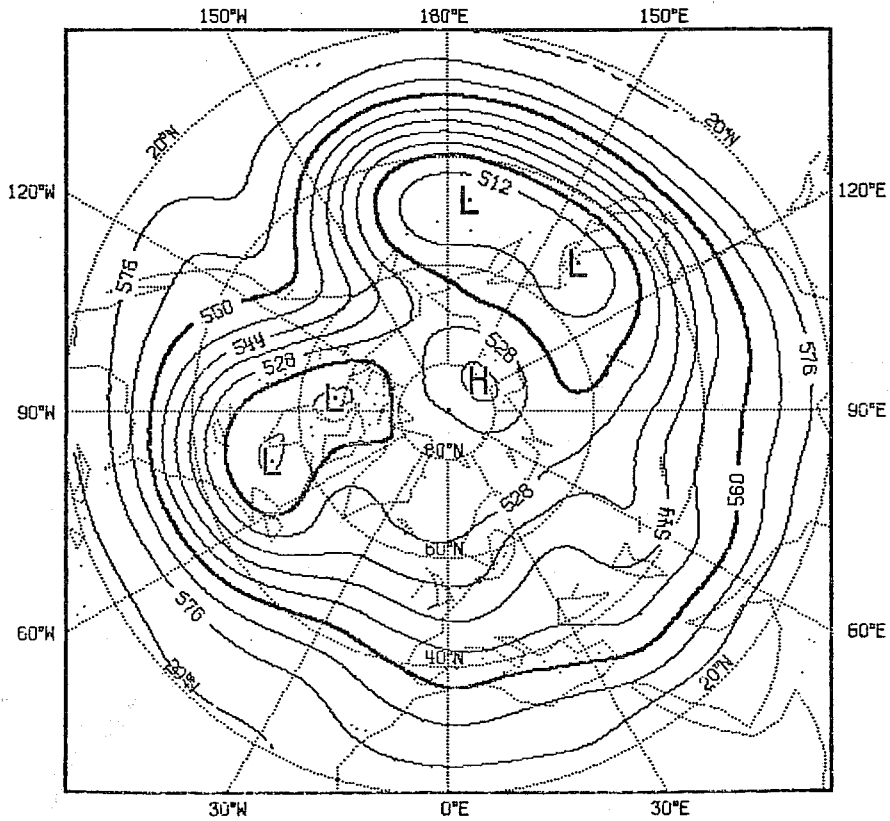NMC DAYS 1.0 TO30.0 1 (1957/ 1/ 2 OGMT) 500 MB INT=8 DKM

$^Z500$ mb

N48L9-E4
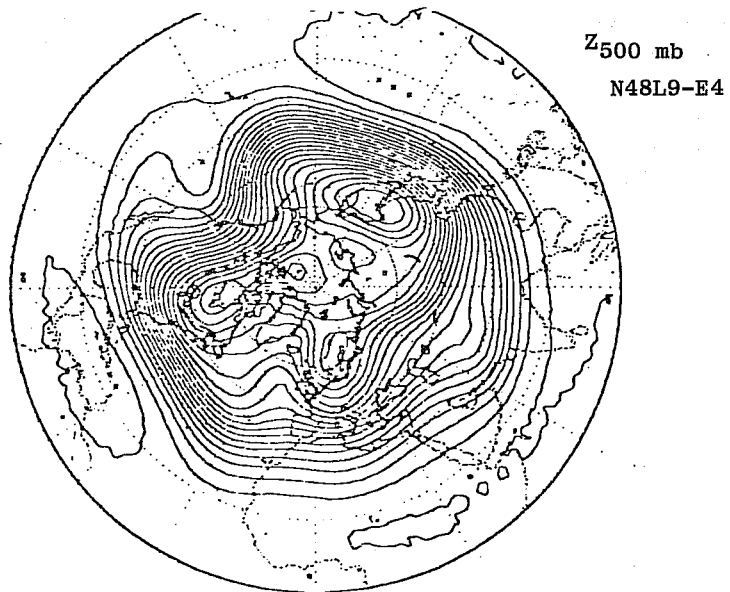
Fig. 15 Northern Hemisphere 30 day mean geopotential
fields for verifying analysis (top) and GFDL
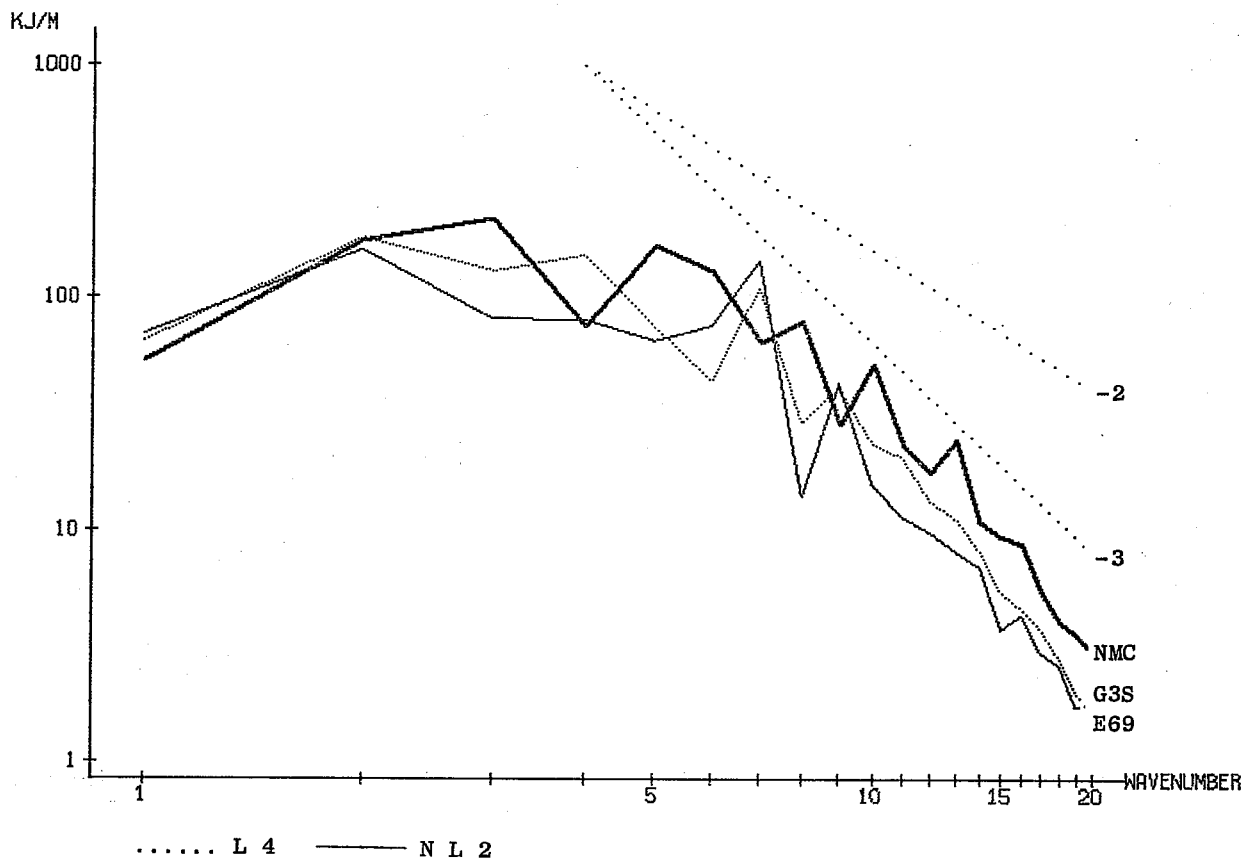forecast (bottom) of the 1.1.77.

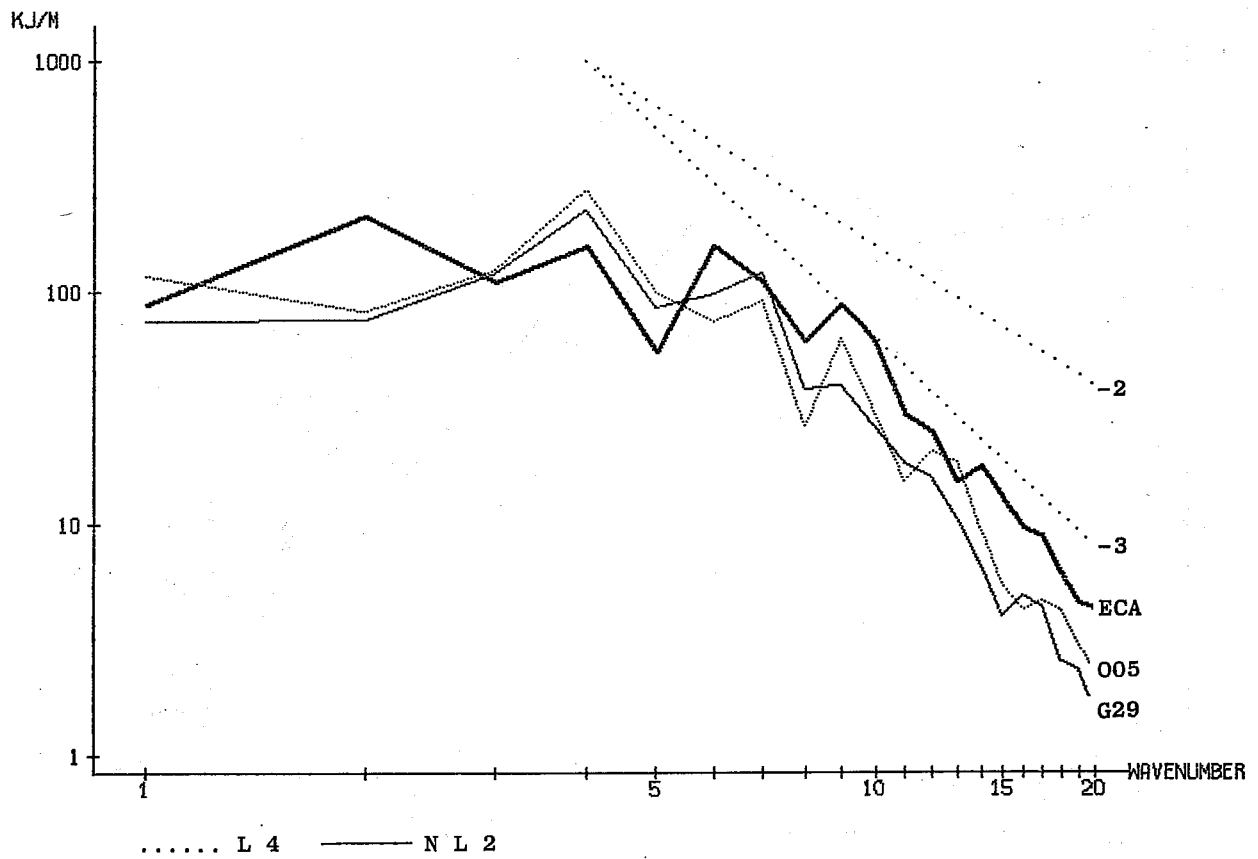Fig. 16b As for Fig. 16a but for 1.3.65.
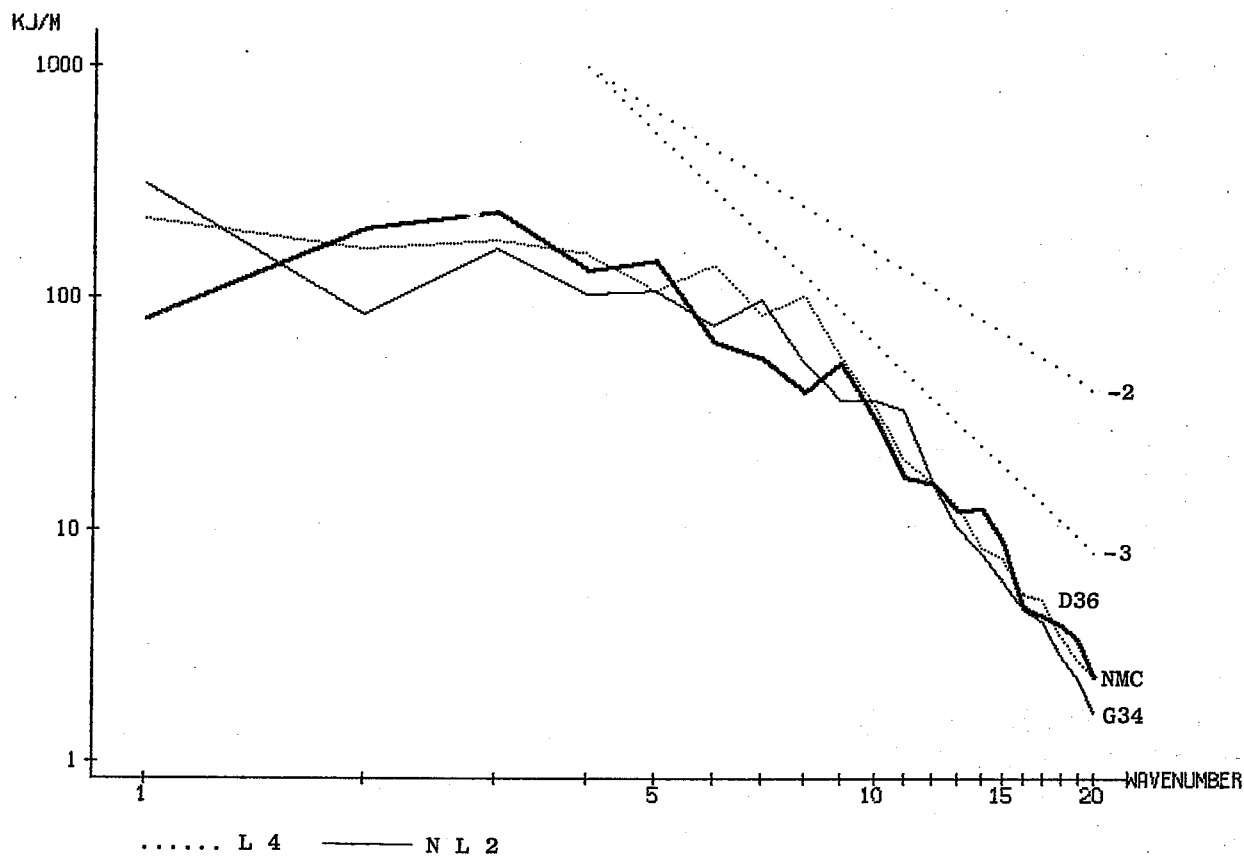
Fig. 16d   As for Fig. 16a but for 5.4.81.

Fig. 17 As for Fig. 16a but for the second half of the 30 day forecasts from 1.1.77.